Anti-Stokes laser-induced internal cooling of Yb^{3+}-doped glasses

J. Fernández,[1,2] A. Mendioroz,[1] A. J. García,[1] R. Balda,[1,2] and J. L. Adam[3]
[1]*Departamento de Física Aplicada I, Escuela Superior de Ingenieros, Alda. Urquijo, 48013 Bilbao, Spain*
[2]*Centro mixto CSIC-UPVIEHU, Escuela Superior de Ingenieros, Alda. Urquijo, 48013 Bilbao, Spain*
[3]*Laboratoire de Verres et Ceramiques, Université de Rennes, Cedex, France*
(Received 12 August 1999)

Anti-Stokes cooling between room temperature and 77 K in a fluorochloride glass (CNBZn) and a fluoride glass (BIG) doped with 1 mol % of YbF_3 has been demonstrated by using collinear photothermal deflection and conventional laser excitation spectroscopies under high photon irradiances. The cooling efficiency for CNBZn glass which is ~2.0% relative to the absorbed laser power at 1010 nm and 300 K falls about 20% at 77 K. The cooling efficiency for BIG glass was only ~0.6% at room temperature. A model accounting for the photon-ion-phonon interaction is in good agreement with the observed temperature dependence of the cooling process and shows its relation with the vibrational properties of the material.

I. INTRODUCTION

Since A. Kastler proposed in the middle of this century that optical cooling of rare-earth-doped crystals could result from anti-Stokes emission, many attempts have been made to demonstrate this effect. However, it was only recently that net optical cooling of a solid was shown in an Yb^{3+}-doped fluorozirconate glass.[1] A year later, laser cooling in vacuo below room temperature was reported by the same research group in an Yb^{3+}-doped fiber made out of the same material,[2] whereas in a subsequent paper internal laser cooling between 100 and 300 K was measured in the same Yb^{3+}-doped bulk glass.[3] The measured cooling efficiencies (cooling power versus absorbed laser power) were around 1% and did not depend on temperature. A characteristic behavior of the experimental data was that there was always some kind of maximum in the cooling region, namely, that cooling efficiencies did not depend linearly with the laser wavelength, as the authors expected, but instead, fell below the theoretical expectation at a given wavelength. This behavior was attributed by the authors to spurious heating effects due to broadband absorption of the pump light. In a more recent paper,[4] the authors have presented an assessment of the optical cooling potential of two fluoride and one phosphate glasses taking into account the temperature dependence of the absorption and luminescence spectra. The cooling efficiencies were calculated as a function of temperature at pumping wavelengths corresponding to an absorption coefficient of $10^{-3}\,cm^{-1}$.

In this work, we present experimental evidences of laser cooling in two bulk Yb^{3+}-doped fluorochloride and fluoride glasses. These results have been obtained by using two different techniques: collinear photothermal deflection spectroscopy and conventional laser excitation spectroscopy performed under the same high photon irradiances. The photothermal measurements give similar results to those found in fluorozirconate glass and show similar cooling efficiencies.[3] However, the spectroscopic results clearly reveal that the cooling range is restricted to a narrow spectral region which depends on the phonon density of states of the material. Moreover, the thermal dependence of the additional fluorescence which appears in the excitation spectra as a consequence of cooling, makes clear that the cooling efficiency is a function of temperature. Together with the experimental results we present a simplified model which gives an explanation about the origin of laser cooling in Yb^{3+}-doped glasses as well as its temperature dependence.

II. EXPERIMENT

Two samples of CNBZn glass (CdF_2-$CdCl_2$-NaF-BaF_2-$BaCl_2$-ZnF_2) and BIG glass (BaF_2-InF_3-GaF_3-ZnF_2-LuF_3-GdF_3) doped with 1 mol % of YbF_3 were investigated. The samples of dimensions $2\times8\times10$ mm were suspended from a silk wire cross inside a cryostat evacuated to $\sim10^{-2}$ mbars to improve thermal isolation. The beam of a tunable ($\lambda=905$ to 1090 nm) cw titanium-sapphire ring laser (8-GHz bandwidth) which entered the sample perpendicularly to the center of the 2×8 mm face was modulated at 1.24 Hz by means of a mechanical chopper. A fraction of the incident power was utilized for signal normalization. A co-propagating helium-neon probe laser beam ($\lambda=632.8$ nm) was co-aligned with the pump beam through a dichroic element. Both pump and probe co-propagating beams were focused into the middle of the sample with diameters of ~100 μm and ~60 μm, respectively. After leaving the sample, the beams passed through a second identical lens separated from the first one by a distance twice the focal length (5 cm) to avoid high divergence of the emerging beams. A second dichroic beam splitter deviated the pumping beam to a pyroelectric detector which measured the transmitted pumping power. Before reaching a quadrant position detector the probe beam passed through an interference filter to eliminate residual pumping radiation. The excitation spectra were measured with the same configuration by collecting the fluorescence at a right angle from the focused area of the pumping beam by means of a collimating lens, and focusing it with a second lens at the 100-μm entrance slit of a 0.22-m monochromator provided with an extended infrared photomultiplier. Lock-in detection was used in both experiments. Ther-

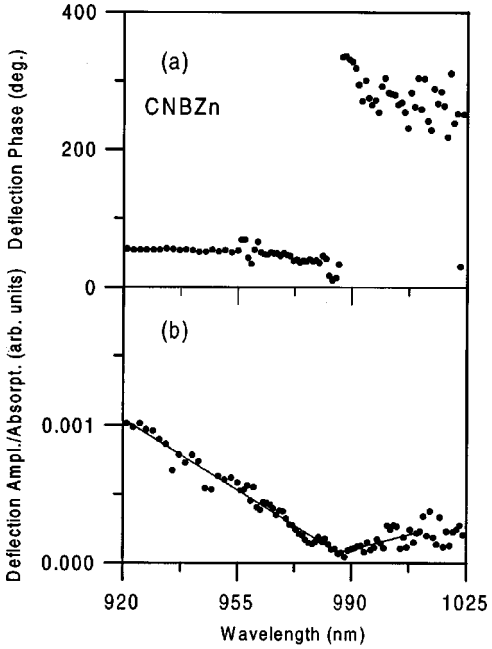

FIG. 1. (a) Phase of the photothermal deflection signal and (b) photothermal deflection amplitude (normalized by the incident laser power) divided by the absorption of the CNBZn glass sample at each wavelength, measured with the lock-in amplifier.

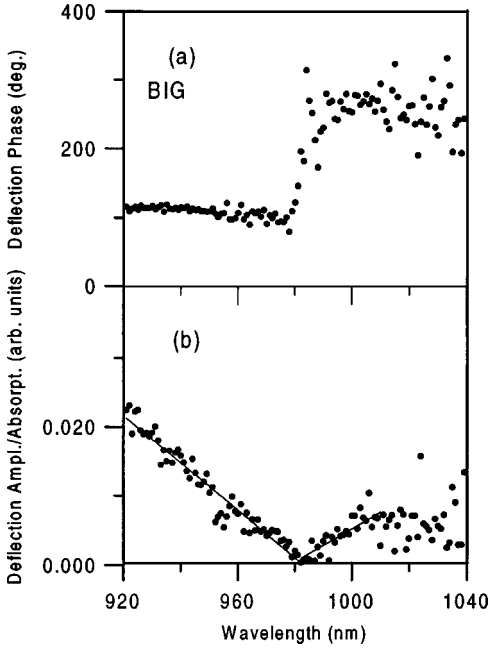

FIG. 2. (a) Phase of the photothermal deflection signal and (b) photothermal deflection amplitude (normalized by the incident laser power) divided by the absorption of the BIG glass sample at each wavelength, measured with the lock-in amplifier.

mal deflection waveforms were detected by using a digital scope.

In this collinear configuration, the amplitude of the angular deviation of the probe beam is always proportional to the amount of heat the sample exchanges, whatever its optical or thermal properties are.[5] This fact allows to relate the amplitude of the deflection at each wavelength to the typical relaxation parameters of the Yb^{3+} ions after the absorption of the pumping radiation, in particular to the quantum efficiency (QE) of the $^2F_{5/2} \rightarrow {}^2F_{7/2}$ transition, by considering the Yb^{3+} ion as a two level system.[6]

III. PHOTOTHERMAL QUANTUM EFFICIENCY MEASUREMENTS

The room-temperature photothermal deflection signal waveforms of the CNBZn glass were recorded in the scope for different pumping wavelengths. The zero signal occurs around 988 nm. The lock-in phase and amplitude of the photothermal deflection, normalized by the absorption, are displayed in Fig. 1 as a function of the pumping wavelength. As predicted by theory,[7] a neat change of about 180°, can be observed during the transition from the heating to the cooling region [Fig. 1(a)]. The QE in the heating region as measured from the photothermal amplitude and absorption[5,6] was 0.996 and the one at the beginning of the cooling region (from 988 to 1010 nm), 1.016. Therefore the cooling efficiency estimated by using the QE measurements is about 2.0%. Figures 2(a), and (b) show the corresponding results for the BIG glass. In this case, the zero photothermal deflection signal occurs at 983 nm and the estimated cooling efficiency (983–1010-nm region) was only 0.6%. It is worthy to notice the nonlinear dependence of the photothermal deflection amplitude with the pumping wavelength in the whole cooling region. This behavior impedes photothermal QE measurements at wavelengths longer than 1010 nm. As we shall see in the next section, this broad peak formed by the photothermal deflection approximately resembles the one observed for the excess of luminescence associated with cooling, thus confirming the nonlinear behavior of this process.

IV. EXCITATION SPECTRA

To further investigate the origin of the observed cooling, we performed excitation measurements in both samples at different pumping photon irradiances and temperatures by keeping the system in the same conditions. As an example, Fig. 3(a) shows the excitation spectra measured at 225 K for the CNBZn glass collecting the luminescence at 1040 nm (at the end of the cooling zone) and at two different pumping irradiances, 880 and 150 mW. Figure 3(b) displays the normalized difference of both spectra. As we can see, except for the zone around the main absorption peak where an accurate difference is difficult to obtain (probably due to some saturation in the spectrum taken at high irradiances), the difference mainly consists of a broad peak [shaded region in Fig. 3(b)] which covers the spectral range where cooling occurs. This new peak must correspond to the excess of fluorescence produced as a consequence of the cooling process which allows for an additional population of the excited state in this region. This means that at high photon irradiances, other than first-order processes are playing a principal role in this spectral range. In the next section a simple model in which an Yb^{3+} ion in its ground state absorbs an incident photon and a phonon of the glass matrix and goes up to the excited state is given as a plausible cooling mechanism.

The dependence with pumping power of the broad peak integrated intensity, which corresponds to the cooling luminescence, is close to linearity whereas it shows a nonlinear

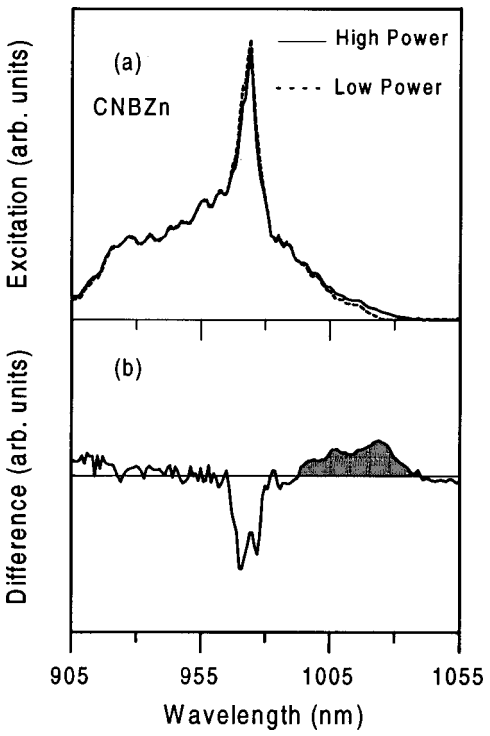

FIG. 3. (a) High power (solid line) and low power (dashed line) excitation spectra recorded at 1040 nm and 225 K in CNBZn glass. (b) Difference between the high and low power spectra. The shaded area corresponds to the cooling luminescence.

temperature dependence. Figures 4 and 5 show, respectively, for CNBZn and BIG glasses, the temperature dependence of both the integrated intensity of the peak and its first moment (centroid of the peak). As we shall see in the next section, the model we propose is able to account for these temperature dependences.

V. A MODEL FOR ANTI-STOKES COOLING

In order to estimate the probability per unit time of such a second-order process let us consider our physical system described by the Hamiltonian

$$H = H^{\text{ion}} + H^{\text{ph}} + H^{\text{em}} + V^{\text{ion-em}} + V^{\text{ion-ph}}, \tag{1}$$

where

$$H^{\text{ion}} = \hbar\omega_0 a^+ a$$

is the Hamiltonian of the ion electronic levels being $\hbar\omega_0$ the energy difference between the optically active energy levels of the dopant ion (considered as a two level ion) and $a^+(a)$ the creation (annihilation) operator of an electronic excitation;

$$H^{\text{ph}} = \sum_q \hbar\omega_q b_q^+ b_q$$

is the phonon field Hamiltonian with ω_q the phonon frecuency and $b_q^+(b_q)$ the creation (annihilation) operator of a phonon in mode q;

$$H^{\text{em}} = \hbar\omega_L c^+ c$$

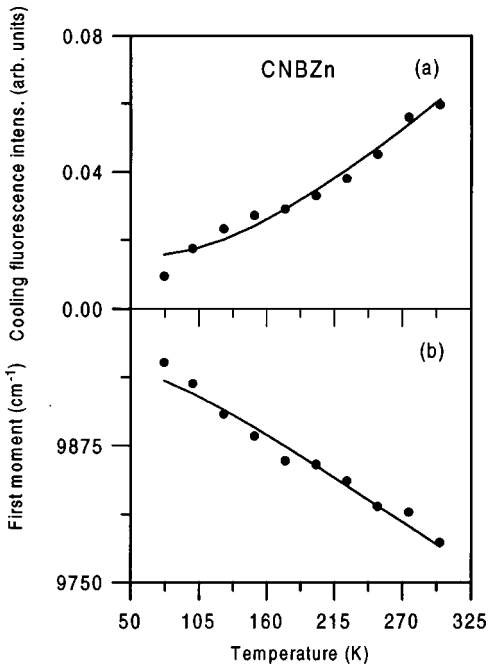

FIG. 4. (a) Experimental cooling fluorescence integrated intensities as a function of temperature (dots) and fitting to Eq. (13) (solid line) for CNBZn glass. (b) Experimental values of the first moment of the cooling fluorescence band (dots) and fitting to Eq. (15) (solid line) for CNBZn glass.

is the electromagnetic laser field with ω_L the laser frequency and $c^+(c)$ the creation (annihilation) operator of a photon;

$$V^{\text{ion-em}} = -\hat{e}_L \cdot \mu \sqrt{\frac{\hbar\omega_L}{2\varepsilon_0 V}}(a^+ + a)(c^+ + c)$$

is the ion-photon interaction Hamiltonian, $\hat{e}_L$ being the po-

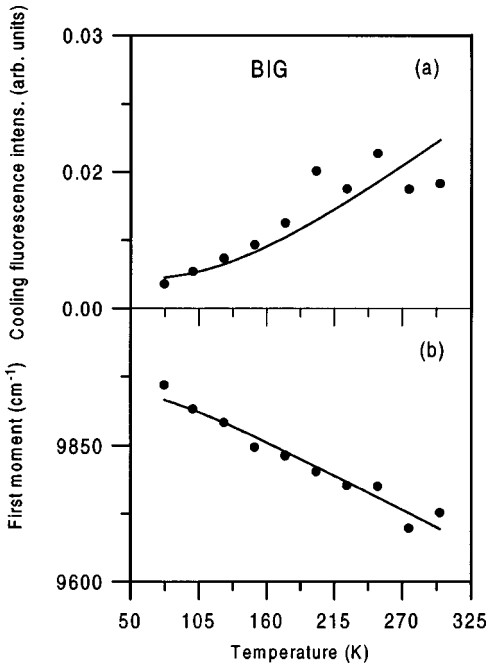

FIG. 5. (a) Experimental cooling fluorescence integrated intensities as a function of temperature (dots) and fitting to Eq. (13) (solid line) for BIG glass. (b) Experimental values of the first moment of the cooling fluorescence band (dots) and fitting to Eq. (15) (solid line) for BIG glass.

larization vector of the photon, μ the dipole moment of the electronic transition, ε_0 the vacuum permittivity, and V the interacting volume;

$$V^{\text{ion-ph}}=\Lambda\sqrt{\frac{\hbar\omega_q}{2\rho\nu^2}}a^+a(b_q-b_q^+)$$

is the ion-phonon interaction Hamiltonian, where Λ is the ion-phonon coupling constant, ν is the sound velocity, and ρ the mass density.

The probability per unit time of a process in which the ion in its ground state absorbs an incident photon and a phonon and goes up to the excited state can be evaluated by using the perturbation theory. This kind of processes appears in the second-order term of the perturbation expansion. The transition probability is given by Fermi's golden rule:

$$w=\sum_f w_{fi}=\frac{2\pi}{\hbar}\sum_f |t_{fi}|^2\delta(E_f-E_i), \tag{2}$$

where E_i and E_f are, respectively, the initial and final energies of the system. The t matrix admits a perturbative expansion given by

$$t_{fi}=\langle f|V_{\text{int}}|i\rangle+\sum_m\frac{\langle f|V_{\text{int}}|m\rangle\langle m|V_{\text{int}}|i\rangle}{E_i^T-E_m^T}+\sum_{m,n}\frac{\langle f|V_{\text{int}}|m\rangle\langle m|V_{\text{int}}|n\rangle\langle n|V_{\text{int}}|i\rangle}{(E_i^T-E_m^T)(E_i^T-E_n^T)}+\cdots \tag{3}$$

with $V_{\text{int}}=V^{\text{ion-em}}+V^{\text{ion-ph}}$. The summation on m and n includes all the intermediate phonon and photon states.

We are interested in the calculation of the transition probability W_{fi} between initial $|i\rangle=|a,n,n_q\rangle$ and final $|f\rangle=|b,0,0\rangle$ states of our system, where the first ket element, a, refers to the ion state, the second one, n, to the photon occupation number, and the third one, to the phonon occupation number. This type of processes only appears at second order in the perturbation theory expansion of the t matrix, and the calculation, though easy, is too lengthy to be presented here and will be given elsewhere. The contribution of these processes to the transition probability is given by

$$W=\sum_f W_{fi}=\frac{2\pi}{\hbar}\left(\frac{\omega_0}{\omega_L}\right)^2\sum_q\left(\frac{gD_q}{\hbar\omega_q}\right)^2\times nn_q\delta(-\hbar\omega_0+\hbar\omega_L+\hbar\omega_q) \tag{4}$$

where

$$g^2=\frac{(\hat{e}_L\cdot\mu)^2}{2\varepsilon_0 V}\hbar\omega_L,\text{and}\ \ D_q^2=\Lambda^2\frac{\hbar\omega_q}{2\rho\nu^2} \tag{5}$$

In order to evaluate the summation on the phonon modes in Eq. (4), we must introduce the phonon density of states $P(E)$. In terms of this distribution function, the transition probability can be expressed in the following way:

$$W=\frac{2\pi}{\hbar}\left(\frac{\omega_0}{\omega_L}\right)^2 g^2 n\frac{\Lambda^2}{2\rho\nu^2}\int_{E_{\min}}^{E_{\max}}dE P(E)\frac{n(E)}{E}\delta(-\hbar\omega_0+\hbar\omega_L+E) \tag{6}$$

which after integration gives

$$W=\pi\frac{(\hat{e}_L\cdot\mu)^2\Lambda^2 n}{2\varepsilon_0 V\rho\nu^2}\frac{\omega_0^2}{\omega_L}\frac{P(\hbar\omega_0-\hbar\omega_L)f(\hbar\omega_0-\hbar\omega_L)}{\hbar\omega_0-\hbar\omega_L},\quad \text{if}\ \ \hbar\omega_0>\hbar\omega_L. \tag{7}$$

In this expression, n is the photon density of the incident beam, f is the Bose-Einstein function, and P is the phonon density of states.

Raman and infrared absorption measurements performed on CNBZn glass powder showed a complex broad band centered around 300 cm^{-1} which may be attributed to Cd-Cl (250 cm^{-1}) and Cd-F (370 cm^{-1}) vibrational modes.[8] Therefore a Gaussian-like function centered around 370 cm^{-1}, the higher energy band, was selected as a plausible function for the phonon density of states. In order to avoid a divergence in the transition probability at the resonance $\hbar\omega_0=\hbar\omega_L$, the Gaussian function was scaled by the Debye distribution function in such a way that at low phonon energies the distribution function resembles the Debye one, whereas it is close to a Gaussian at the center of the distribution. This choice avoids the introduction of a cutoff at low phonon frequencies and therefore the introduction of unnecessary parameters in the model. The form of the selected function is

$$P(E)=CE^2\exp\left[-\left(\frac{E-\overline{E}}{\Gamma}\right)^2\right], \tag{8}$$

where $E=\hbar\omega_0-\hbar\omega_L$ is the phonon energy, $\overline{E}=\hbar\overline{\omega}$ is the energy at the center of the distribution, Γ its width ($\sim$100 cm^{-1}), and C an adequate normalization constant.

In the case of BIG glass, on the basis of Raman measurements in similar compounds,[9] the center of the Gaussian function representing the phonon density of states was taken at 510 cm^{-1}, and $\Gamma\sim 100\,\text{cm}^{-1}$.

With this distribution function, expression (7) becomes

$$W=C\pi\frac{(\hat{e}_L\cdot\mu)^2\Lambda^2 n}{2\varepsilon_0 V\rho\nu^2}\frac{(\hbar\omega_0-\hbar\omega_L)\omega_0^2}{\omega_L}\times\exp\left[-\left(\frac{\hbar\omega_0-\hbar\omega_L-\hbar\overline{\omega}}{\Gamma}\right)^2\right]f(\hbar\omega_0-\hbar\omega_L), \tag{9}$$

if $\hbar\omega_0>\hbar\omega_L$.

The intensity of the additional fluorescence is proportional to the population excess of the fluorescent level produced by these second-order processes and the probability for radiative transition to the ground state. Therefore, taking the emitting level QE as one, the temperature dependence of the integrated cooling fluorescence can be determined by comparing the experimental data with the expression

$$I(T)\sim\int W(\omega_L,T)d\omega_L. \tag{10}$$

We can integrate on the absorbed phonon energy, $E=\hbar\omega_0-\hbar\omega_L$, at each pumping frequency. The lower limit of the integral is zero whereas we can take the Debye energy representing the maximum phonon energy present in the material as the upper limit. In any case, the value of the integral is quite insensitive to the upper limit as long as we are far from $E=\hbar\omega_0$, as it is the case.

Substituting expression (9) in Eq. (10) gives

$$I(T)\sim \int_{\hbar\omega_0-\hbar\omega_D}^{\hbar\omega_0} \frac{\omega_0-\omega_L}{\omega_L} \times \exp\left[-\left(\frac{\omega_0-\omega_L-\overline{\omega}}{\Delta\omega}\right)^2\right] f(\hbar\omega_0-\hbar\omega_L)\,d\omega_L, \tag{11}$$

where $\hbar\overline{\omega}=\overline{E}$ and $\hbar\Delta\omega=\Gamma$. Introducing the variable $x=\omega_0-\omega_L$ we finally obtain

$$I(T)\sim \int_0^{\omega_D} \frac{x}{\omega_0-x}\exp\left[-\left(\frac{x-\overline{\omega}}{\Delta\omega}\right)^2\right]\frac{1}{\exp(x/k_BT)-1}\,dx, \tag{12}$$

where ω_D is the Debye frequency.

In order to compare the results of the numerical evaluation of the integrated intensity [expression (12)] with the experimental data, we have included the effect of inhomogeneous broadening by adding a constant background independent of temperature:

$$\mathcal{I}(T)=a+bI(T), \tag{13}$$

where a and b are constants.

Before giving a comparison between the temperature dependence of the measured excess of luminescence, associated with the cooling process, and expression (13), it is worth discussing another important experimental fact, mentioned in Sec. IV, which is the displacement of the transition peak position with temperature.

In order to account for the temperature dependence of the transition peak energy we need to include an additional term in the expansion of the ion-phonon interaction potential[10]

$$V^{\text{ion-ph}}=V_1\varepsilon+V_2\varepsilon^2. \tag{14}$$

The displacement difference ΔE_{ba} between states a and b due to this interaction is then given by

$$\Delta E_{ba}(T)\sim \int_0^{E_D}\frac{E^2}{\exp(E/kT)-1}\exp\left[-\left(\frac{E-\overline{E}}{\Delta E}\right)^2\right]dE. \tag{15}$$

VI. COMPARISON WITH EXPERIMENTAL RESULTS

Figures 4(a) and 5(a) show the integrated intensity of the cooling fluorescence peak as a function of temperature for both glasses. The continuous line is the fitting with the theoretical model given by Eq. (13). The only parameters used in this fitting are the constants in Eq. (13) accounting for the inhomogeneous broadening. Figures 4(b) and 5(b) present the comparison between the experimental displacement of the fluorescence peak as a function of temperature and the theoretical prediction given by Eq. (15).

As we can see, the agreement between experimental results and theory is very good and supports not only the model hypothesis about the kind of processes involved, but also the distribution function used for the phonon energies. Moreover, if we compare the relative integrated intensities at different temperatures we can have a real picture about the temperature dependence of the cooling efficiency of the material. Our experimental results in these glasses show it is possible to cool an internal volume from room temperature down to 70 K but with a penalty of about a 20% in the cooling efficiency (cooling efficiency is defined as the ratio of the integrated cooling fluorescence peak to the integrated intensity of the high power excitation spectrum without the cooling peak contribution).

It is worthy to mention the quite good agreement between the room-temperature cooling efficiencies obtained by using photothermal QE measurements and the ones obtained by measuring the fluorescence excess from the excitation spectra. In the former case efficiencies of 2 and 0.6%, respectively, were found for CNBZn and BIG glasses, whereas in the second case values of 3 and 1%, respectively were obtained for the same samples.

In conclusion, we can state that anti-Stokes cooling in solids is dependent on the phonon density of states of the system as well as on the ion-phonon coupling constant. Appropriate values of the mean phonon energies and of the ion-phonon coupling constants may lead to the cooling process in presence of a high enough photon irradiance.

From a fundamental point of view these results open a wide field for searching and tailoring materials in which these kinds of processes could be enhanced, and their physical grounds, which certainly involve the phonon density of states and the ion-phonon coupling strength, be better understood.

ACKNOWLEDGMENTS

This work has been supported by the Basque Country University (G21/98), Spanish Government CICYT (Ref. MAT97-1009), (DGICYT Ref. PB95-0512), (HF-1998-0154), and Basque Country Government (PI97/99).

[1] R. I. Epstein, M. I. Buchwald, B. C. Edwards, T. R. Gosnell, and C. E. Mungan, Nature (London) **377**, 500 (1995).
[2] C. E. Mungan, M. I. Buchwald, B. C. Edwards, R. I. Epstein, and T. R. Gosnell, Phys. Rev. Lett. **78**, 1030 (1997).
[3] C. E. Mungan, M. I. Buchwald, B. C. Edwards, R. I. Epstein, and T. R. Gosnell, Appl. Phys. Lett. **71**, 1458 (1997).
[4] Gang Lei *et al.*, IEEE J. Quantum Electron. **34**, 1839 (1998).
[5] A. Salazar, A. Sánchez-Lavega, and J. Fernández, J. Appl. Phys. **74**, 1539 (1993).
[6] J. Etxebarria and J. Fernández, J. Phys. C **16**, 3803 (1983).
[7] W. B. Jackson, N. M. Amer, A. C. Boccara, and D. Fournier, Appl. Opt. **20**, 1333 (1981).
[8] J. L. Adam (unpublished).
[9] R. M. Almeida, J. C. Pereira, Y. Messaddeq, and M. A. Aegerter, J. Non-Cryst. Solids **161**, 105 (1993).
[10] B. Henderson and G. F. Imbusch, *Optical Spectroscopy of Inorganic Solids* (Oxford Science, 1989).